Delft University of Technology

Stochastic Aerospace Systems Practical
AE4304P

Assignment: Asymmetrical aircraft responses for a rigid aircraft in asymmetrical atmospheric turbulence

Author:
Mayukh Sarkar (5219507)

March 19, 2021

Contents

List of Figures

List of Tables

Chapter 1

Introduction

An aircraft's motion and trajectory are dependent on the local atmospheric properties. One of those properties can be attributed to atmospheric turbulence. It is caused by the irregular motion of air-particles varying in both speed and direction. Turbulence can vary in different conditions like near the ground, due to clouds or in the clear atmosphere, and also due to the presence of natural barriers like mountains. While modeling atmospheric turbulence certain assumptions[1] are taken into account such as:

- Turbulence is a random process with Gaussian distribution.
- Atmospheric turbulence is a stationary process.
- Atmospheric turbulence is homogeneous throughout the flight path.
- Atmospheric turbulence is an isotropic process.

The turbulence can be decomposed into longitudinal gust $\bar{u_g}$, lateral gust $\bar{v_g}$ and vertical gust $\bar{w_g}$. In this report, we analyze asymmetric aircraft responses to the lateral and vertical gust components. The vertical component accelerates the aircraft vertically and can give rise to pitching moments. The lateral component acts on the vertical tail and fuselage and can give rise to rolling and yawing motions. These abrupt motions can make the aircraft unstable thus making it difficult to control. Also, they may induce pilot fatigue and passenger discomfort. Violent turbulence can also cause structural damage to the aircraft. The conditions provided for the analysis are as follows:

$$L_g = 150\ m \qquad \sigma_{v_g} = 1\ m/s \qquad \sigma_{w_g} = 2\ m/s \tag{1.1}$$

The analysis is made using the Dryden power spectral model[1]. For comparison two aircraft models are used, a full model and a reduced model considering the dutch roll. The upcoming chapters focus on the stability analysis, time response, spectral analysis, and variances of the aircraft responses for the two models due to the vertical and lateral gust components. The findings are described in the conclusion chapter.

Chapter 2

Stability Analysis

This chapter provides an insight into the stability analysis of the aircraft models used in the assignment. For the stability analysis two models, one having a full set of motion equations and another reduced model that approximates the dutch roll behavior has been used. The aircraft's response to the simulations are for both lateral and vertical turbulence simultaneously are determined by using the following conditions:

$$L_g = 150\ m \qquad \sigma_{v_g} = 1\ m/s \qquad \sigma_{w_g} = 2\ m/s \tag{2.1}$$

The state space for the full model is represented by the equation[2]:

$$\dot{X} = AX + BU \tag{2.2}$$

The state vector is given by X and the control input is given by U as described below:

$$X = \begin{bmatrix} \beta & \varphi & \frac{pb}{2V} & \frac{rb}{2V} & \hat{u_g} & \hat{u_g}^* & \alpha_g & \alpha_g^* & \beta_g & \beta_g^* \end{bmatrix}^T \tag{2.3}$$

$$U = \begin{bmatrix} \delta_a & \delta_r & w_1 & w_2 & w_3 \end{bmatrix}^T \tag{2.4}$$

The matrix A is given by :

$$A = \begin{bmatrix} y_\beta & y_\phi & y_p & y_r & 0 & 0 & 0 & 0 & y_{\beta_g} & 0 \\ 0 & 0 & \frac{2V}{b} & 0 & 0 & 0 & 0 & 0 & 0 & 0 \\ l_\beta & 0 & l_p & l_r & l_{u_g} & 0 & l_{\alpha_g} & 0 & l_{\beta_g} & 0 \\ n_\beta & 0 & n_p & n_r & n_{u_g} & 0 & n_{\alpha_g} & 0 & n_{\beta_g} & 0 \\ 0 & 0 & 0 & 0 & 0 & 1 & 0 & 0 & 0 & 0 \\ 0 & 0 & 0 & 0 & -(\frac{V}{L_g})^2 \frac{1}{\tau_1 \tau_2} & -\frac{\tau_1+\tau_2}{\tau_1 \tau_2} \frac{V}{L_g} & 0 & 0 & 0 & 0 \\ 0 & 0 & 0 & 0 & 0 & 0 & 0 & 1 & 0 & 0 \\ 0 & 0 & 0 & 0 & 0 & 0 & -(\frac{V}{L_g})^2 \frac{1}{\tau_4 \tau_5} & -\frac{\tau_4+\tau_5}{\tau_4 \tau_5} \frac{V}{L_g} & 0 & 0 \\ 0 & 0 & 0 & 0 & 0 & 0 & 0 & 0 & 0 & 1 \\ 0 & 0 & 0 & 0 & 0 & 0 & 0 & 0 & -(\frac{V}{L_g})^2 & \frac{-2V}{L_g} \end{bmatrix} \tag{2.5}$$

Substituting the values of the constants into the matrix of Equation 2.5 the following result is obtained:

$$\begin{bmatrix} -0.188 & 0.0927 & -0.0187 & -18.0977 & 0 & 0 & 0 & 0 & -0.188 & 0 \\ 0 & 0 & 18.159 & 0 & 0 & 0 & 0 & 0 & 0 & 0 \\ -0.534 & 0 & -2.026 & 0.9055 & -0.6625 & 0 & -1.621 & 0 & -0.534 & 0 \\ 0.323 & 0 & -0.103 & -0.3211 & 0.0382 & 0 & -0.0816 & 0 & 0.323 & 0 \\ 0 & 0 & 0 & 0 & 0 & 1.0000 & 0 & 0 & 0 & 0 \\ 0 & 0 & 0 & 0 & -11.90 & -9.618 & 0 & 0 & 0 & 0 \\ 0 & 0 & 0 & 0 & 0 & 0 & 0 & 1 & 0 & 0 \\ 0 & 0 & 0 & 0 & 0 & 0 & -33.088 & -15.933 & 0 & 0 \\ 0 & 0 & 0 & 0 & 0 & 0 & 0 & 0 & 0 & 1 \\ 0 & 0 & 0 & 0 & 0 & 0 & 0 & 0 & -0.654 & -1.617 \end{bmatrix} \tag{2.6}$$

Similarly, the matrix B is given by :

$$B = \begin{bmatrix} 0 & y_{\delta_r} & 0 & 0 & 0 \\ 0 & 0 & 0 & 0 & 0 \\ l_{\delta_a} & l_{\delta_r} & 0 & 0 & 0 \\ n_{\delta_a} & n_{\delta_r} & 0 & 0 & 0 \\ 0 & 0 & \frac{\tau_3}{\tau_1\tau_2}\sqrt{\frac{V}{L_g}I_{\hat{u}_g}} & 0 & 0 \\ 0 & 0 & (1-\frac{\tau_3(\tau_1+\tau_2)}{\tau_1\tau_2})\frac{1}{\tau_1\tau_2}\sqrt{(\frac{V}{L_g})^3 I_{\hat{u}_g}} & 0 & 0 \\ 0 & 0 & 0 & \frac{\tau_6}{\tau_4\tau_5}\sqrt{\frac{V}{L_g}I_{\alpha_g}} & 0 \\ 0 & 0 & 0 & (1-\frac{\tau_6(\tau_4+\tau_5)}{\tau_4\tau_5})\frac{1}{\tau_4\tau_5}\sqrt{(\frac{V}{L_g})^3 I_{\alpha_g}} & 0 \\ 0 & 0 & 0 & 0 & \sigma_{\beta_g}\sqrt{\frac{3V}{L_g}} \\ 0 & 0 & 0 & 0 & (1-2\sqrt{3})\sigma_{\beta_g}\sqrt{(\frac{V}{L_g})^3} \end{bmatrix} \tag{2.7}$$

$$B = \begin{bmatrix} 0 & 0.0431 & 0 & 0 & 0 \\ 0 & 0 & 0 & 0 & 0 \\ -1.2590 & 0.2079 & 0 & 0 & 0 \\ -0.0544 & -0.2305 & 0 & 0 & 0 \\ 0 & 0 & 0.0177 & 0 & 0 \\ 0 & 0 & -0.1359 & 0 & 0 \\ 0 & 0 & 0 & 0.0227 & 0 \\ 0 & 0 & 0 & -0.2798 & 0 \\ 0 & 0 & 0 & 0 & 0.0128 \\ 0 & 0 & 0 & 0 & -0.0148 \end{bmatrix} \tag{2.8}$$

The matrix C is constructed using the Matlab function *eye(10,10)* which gives a 10x10 identity matrix. Likewsie the matrix B only contains zeros constructed using the command *zeros(10,5)* which is a 10x5 matrix. The pole-zero map and the eigen values of the above statespace are obtained using the command ss & *pzmap* respectively.

From the pole zero-map in Figure 2.1, it is noted that one eigenvalue lies in the positive

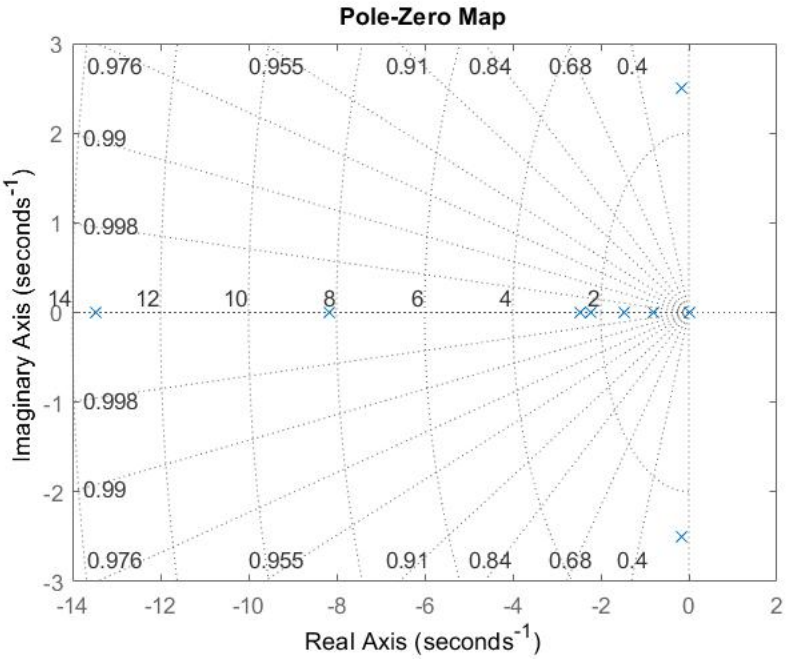

Figure 2.1: Pole-zero map of the full uncontrolled system

right-hand side of the imaginary axis. The eigenvalue 0.0146 makes the whole system unstable. So the value of the gain K_ϕ has to be adjusted to make the system stable.

$$\delta_a = K_\phi \phi + K_p p \tag{2.9}$$

A new value of K_ϕ is chosen as -0.2 which makes the system relatively stable with all the eigenvalues lying on the left-hand negative side of the imaginary axis.No value for the rate of roll gain is introduced as there's no need and the system is already stable. The unstable eigenvalue from Figure 2.1 is now shifted to the left side of the imaginary axis making the system stable. The stable fully controlled system is shown in Figure 2.2. The new state space matrix A is given in Equation 2.

$$\begin{bmatrix} -0.188 & 0.0927 & -0.0187 & -18.097 & 0 & 0 & 0 & 0 & -0.188 & 0 \\ 0 & 0 & 18.158 & 0 & 0 & 0 & 0 & 0 & 0 & 0 \\ -0.534 & -0.252 & -2.0259 & 0.9055 & -0.6625 & 0 & -1.621 & 0 & -0.534 & 0 \\ 0.323 & -0.0109 & -0.1028 & -0.3211 & 0.0382 & 0 & -0.082 & 0 & 0.323 & 0 \\ 0 & 0 & 0 & 0 & 0 & 1.0000 & 0 & 0 & 0 & 0 \\ 0 & 0 & 0 & 0 & -11.9005 & -9.6185 & 0 & 0 & 0 & 0 \\ 0 & 0 & 0 & 0 & 0 & 0 & 0 & 1.0000 & 0 & 0 \\ 0 & 0 & 0 & 0 & 0 & 0 & -33.0875 & -15.9327 & 0 & 0 \\ 0 & 0 & 0 & 0 & 0 & 0 & 0 & 0 & 0 & 1 \\ 0 & 0 & 0 & 0 & 0 & 0 & 0 & 0 & -0.654 & -1.617 \end{bmatrix} \tag{2.10}$$

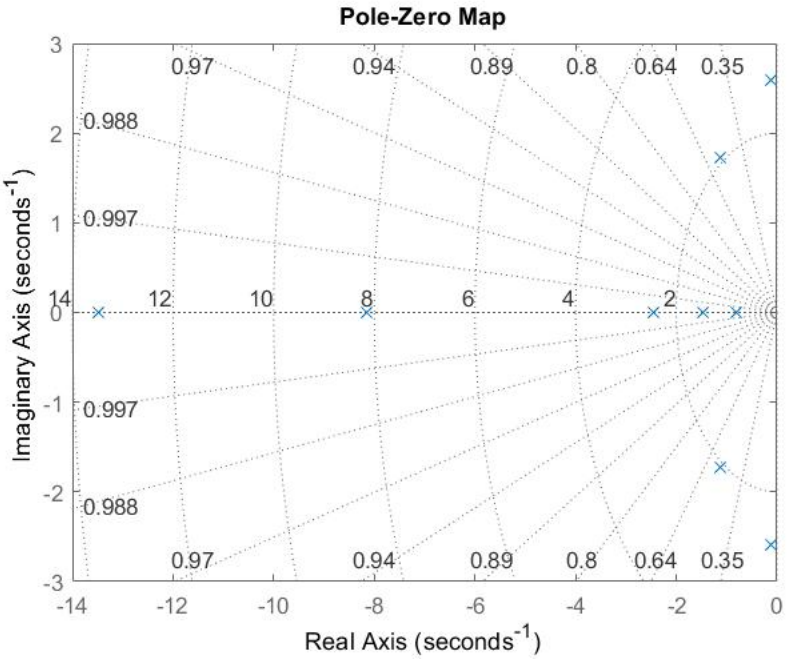

Figure 2.2: Pole-zero map of the full controlled system

The states of the system are reduced to induce a dutch roll like behaviour.This is done by removing the ϕ and $\frac{pb}{2V}$ elements from the state vector X thus simulatnoeusly reducing the A and B matrix.The representations are shown below:

$$\varphi = \frac{pb}{2V} = 0 \tag{2.11}$$

$$X = \begin{bmatrix} \beta & \frac{rb}{2V} & \hat{u_g} & \hat{u_g}^* & \alpha_g & \alpha_g^* & \beta_g & \beta_g^* \end{bmatrix}^T \tag{2.12}$$

$$A_r = \begin{bmatrix} y_\beta & y_r & 0 & 0 & 0 & 0 & y_{\beta_g} & 0 \\ n_\beta & n_r & n_{u_g} & 0 & n_{\alpha_g} & 0 & n_{\beta_g} & 0 \\ 0 & 0 & 0 & 1 & 0 & 0 & 0 & 0 \\ 0 & 0 & 0 & -(\frac{V}{L_g})^2\frac{1}{\tau_1\tau_2} & -\frac{\tau_1+\tau_2}{\tau_1\tau_2}\frac{V}{L_g} & 0 & 0 & 0 \quad 0 \\ 0 & & 0 & 0 & 0 & 0 & 1 & 0 \quad 0 \\ 0 & 0 & 0 & 0 & -(\frac{V}{L_g})^2\frac{1}{\tau_4\tau_5} & -\frac{\tau_4+\tau_5}{\tau_4\tau_5}\frac{V}{L_g} & 0 & 0 \\ 0 & 0 & 0 & 0 & 0 & 0 & 0 & 1 \\ 0 & 0 & 0 & 0 & 0 & 0 & -(\frac{V}{L_g})^2 & \frac{-2V}{L_g} \end{bmatrix}$$

(2.13)

$$B_r = \begin{bmatrix} 0 & y_{\delta_r} & 0 & 0 & 0 \\ n_{\delta_a} & n_{\delta_r} & 0 & 0 & 0 \\ 0 & 0 & \frac{\tau_3}{\tau_1\tau_2}\sqrt{\frac{V}{L_g}I_{\hat{u}_g}} & 0 & 0 \\ 0 & 0 & (1-\frac{\tau_3(\tau_1+\tau_2)}{\tau_1\tau_2})\frac{1}{\tau_1\tau_2}\sqrt{(\frac{V}{L_g})^3 I_{\hat{u}_g}} & 0 & 0 \\ 0 & 0 & 0 & \frac{\tau_6}{\tau_4\tau_5}\sqrt{\frac{V}{L_g}I_{\hat{u}_g}} & 0 \\ 0 & 0 & 0 & (1-\frac{\tau_6(\tau_4+\tau_5)}{\tau_4\tau_5})\frac{1}{\tau_4\tau_5}\sqrt{(\frac{V}{L_g})^3 I_{\hat{u}_g}} & 0 \\ 0 & 0 & 0 & 0 & \sigma_{\beta_g}\sqrt{\frac{3V}{L_g}} \\ 0 & 0 & 0 & 0 & (1-2\sqrt{3})\sigma_{\beta_g}\sqrt{(\frac{V}{L_g})^3} \end{bmatrix}$$

(2.14)

The C matrix is a 8×8 identity matrix constructed using the Matlab command *eye(8,8)* and the D matrix is of the same dimension as the B, is a null matrix constructed using the matlab command *zeros(8,5)*. Substituting the values for all the elements in both A and B matrices , the following are obtained:

$$A_r = \begin{bmatrix} -0.1880 & -18.0977 & 0 & 0 & 0 & 0 & -0.1880 & 0 \\ 0.3229 & -0.3211 & 0.0382 & 0 & -0.0816 & 0 & 0.3229 & 0 \\ 0 & 0 & 0 & 1.0000 & 0 & 0 & 0 & 0 \\ 0 & 0 & -11.9005 & -9.6185 & 0 & 0 & 0 & 0 \\ 0 & 0 & 0 & 0 & 0 & 1.0000 & 0 & 0 \\ 0 & 0 & 0 & 0 & -33.0875 & -15.9327 & 0 & 0 \\ 0 & 0 & 0 & 0 & 0 & 0 & 0 & 1.0000 \\ 0 & 0 & 0 & 0 & 0 & 0 & -0.6539 & -1.6173 \end{bmatrix}$$

(2.15)

$$B_r = \begin{bmatrix} 0 & 0.0431 & 0 & 0 & 0 \\ -0.0544 & -0.2305 & 0 & 0 & 0 \\ 0 & 0 & 0.0177 & 0 & 0 \\ 0 & 0 & -0.1359 & 0 & 0 \\ 0 & 0 & 0 & 0.0227 & 0 \\ 0 & 0 & 0 & -0.2798 & 0 \\ 0 & 0 & 0 & 0 & 0.0128 \\ 0 & 0 & 0 & 0 & -0.0148 \end{bmatrix} \quad (2.16)$$

The pole zero graph Figure 2.3 of the reduced system mentioned above is plotted using the Matlab command *pz*. It is noted that all the eigen values lie on the negative left hand side of the imaginary axis and thus making the whole system stable.An overview of the eigen values for three systems are given below:

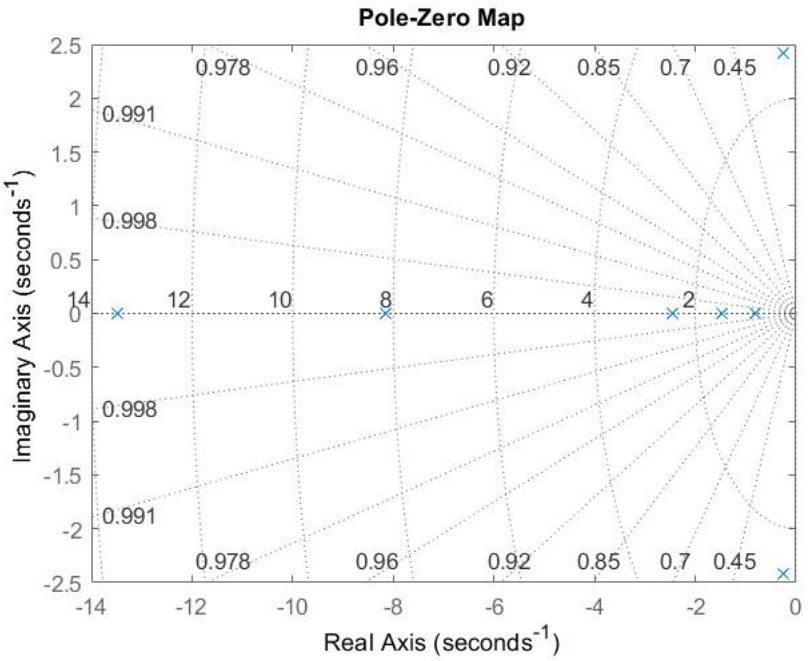

Figure 2.3: Pole-zero map of the reduced system

Eigen Values		
Uncontrolled system	Controlled system	Reduced system
-0.1677+2.5070 i	-0.1313+2.5878 i	-0.2545 + 2.4165i
-0.1677-2.5070 i	-0.1313-2.5878 i	-0.2545 - 2.4165i
-2.2140+0.0000 i	-1.1362+1.7289 i	-1.4584 + 0.0000i
0.0146+0.0000 i	-1.1362-1.7289 i	-8.1601 + 0.0000i
-1.4584+0.0000 i	-1.4584+0.0000 i	-2.4550 + 0.0000i
-8.1601+0.0000 i	-8.1601+0.0000 i	-13.4778 + 0.0000i
-2.4550+0.0000 i	-2.4550+0.0000 i	-0.8087 + 0.0000i
-13.4778+0.0000 i	-13.4778+0.0000 i	-0.8087 + 0.0000i
-0.8087+0.0000 i	-0.8087+0.0000 i	
-0.8087+0.0000 i	-0.8087+0.0000 i	

Table 2.1: Eigen values of the uncontrolled , controlled and reduced systems respectively

Chapter 3

Time-Domain Simulations

The chapter focuses the time domain analysis of the state variables for both the complete and reduced systems to the turbulence.The responses along with the lateral acceleration of the aircraft is taken into account. The lateral acceleration for the both the models are given by:

$$a_y = \frac{d}{dt} V \sin(\beta + \psi) \approx V(\dot{\beta} + \dot{\psi}) \tag{3.1}$$

The controlled state spaces used for the simulations are taken from chapter 2. However to accommodate the lateral acceleration into the system, the C matrix is modified into a 5×10 matrix, with the 5^{th} having the acceleration values. The matrix is shown in Equation 3.3

$$C = \begin{bmatrix} 1 & 0 & 0 & 0 & 0 & 0 & 0 & 0 & 0 & 0 \\ 0 & 1 & 0 & 0 & 0 & 0 & 0 & 0 & 0 & 0 \\ 0 & 0 & 1 & 0 & 0 & 0 & 0 & 0 & 0 & 0 \\ 0 & 0 & 0 & 1 & 0 & 0 & 0 & 0 & 0 & 0 \\ Vy_\beta & Vy_\phi & By_p & V\left(y_r + \left(\frac{2V}{b}\right)\right) & 0 & 0 & 0 & 0 & Vy_{\beta_g} & 0 \end{bmatrix} \tag{3.2}$$

$$C = \begin{bmatrix} 1 & 0 & 0 & 0 & 0 & 0 & 0 & 0 & 0 & 0 \\ 0 & 1 & 0 & 0 & 0 & 0 & 0 & 0 & 0 & 0 \\ 0 & 0 & 1 & 0 & 0 & 0 & 0 & 0 & 0 & 0 \\ 0 & 0 & 0 & 1 & 0 & 0 & 0 & 0 & 0 & 0 \\ -22.8009 & 11.2441 & -0.0008 & 7.3995 & 0 & 0 & 0 & 0 & -22.8009 & 0 \end{bmatrix} \tag{3.3}$$

The systems are simulated over a time period of 100 seconds, taken at an interval of 0.005 (dt) seconds to get the output. The input contains the lateral(v_g) and vertical(w_g) component of the turbulence. The the input matrix are given as :

$$u_v = \begin{bmatrix} nn & nn & nn & v_g & nn \end{bmatrix} \tag{3.4}$$

$$u_w = \begin{bmatrix} nn & nn & nn & nn & w_g \end{bmatrix} \tag{3.5}$$

The values **nn** are 1201×1 array and turbulence are constructed as arrays having the length of the **nn** , randomized and divided by ***dt*** to convert it from continuous-time to discrete-time.The *rand* command is used to produce a white noise-like behavior in the turbulence. So the input matrices are 1201×5 matrices. And the outputs are derived by simulating the controlled and reduced systems against each component of the turbulence and finally adding them up respectively to get the total output for each system against the turbulence. The outputs are determined using the MATLAB function *lsim*. Both the systems are simulated for 100 seconds against each input parameter and the total sum of outputs for each system is

shown in Figure 3.1. The states derived from the from the output are β,φ,$\frac{pb}{2V}$,$\frac{rb}{2V}$, & the lateral acceleration a_y. For the reduced system, the outputs taken into account are β, $\frac{rb}{2V}$ and a_y. All the outputs are shown below in Figure 3.1, Figure 3.2,Figure 3.3,Figure 3.4,Figure 3.5

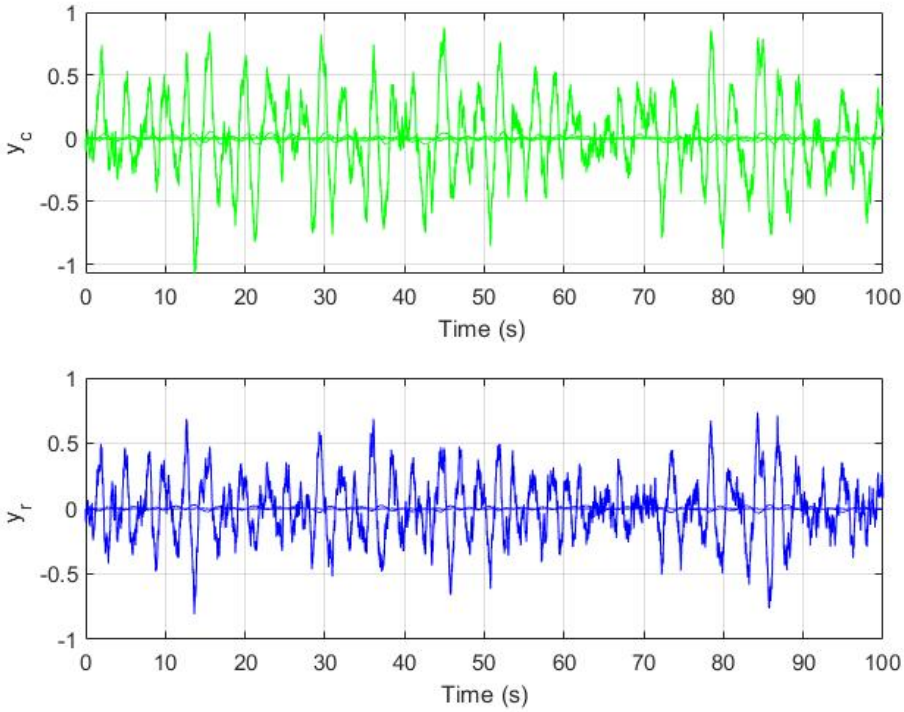

Figure 3.1: Time response of output of the controlled(y_c) & reduced system(y_r)

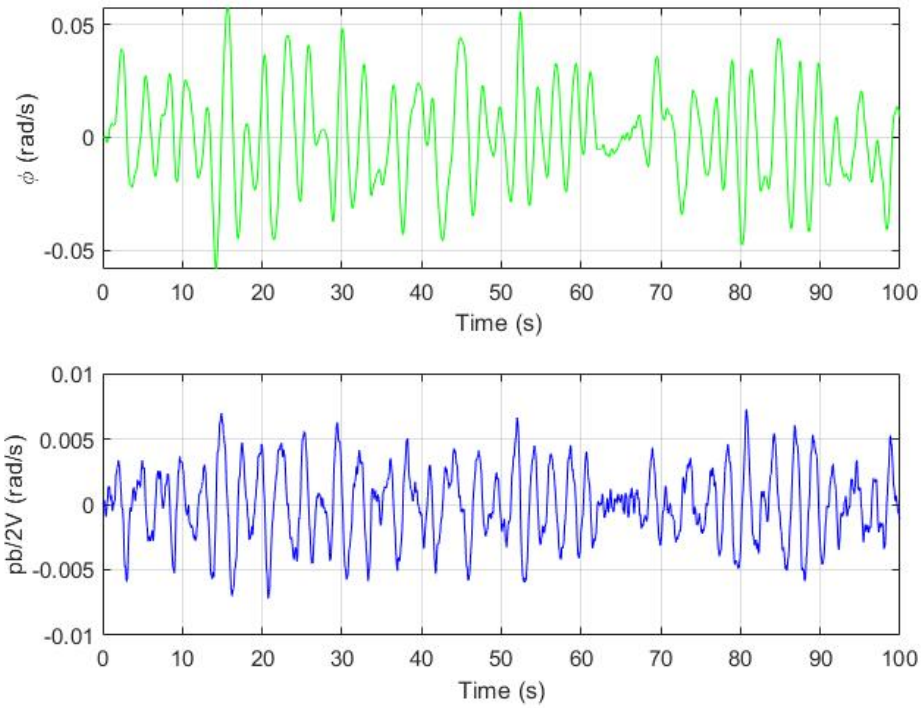

Figure 3.2: Time response of ϕ & $pb/2V$ for the controlled system

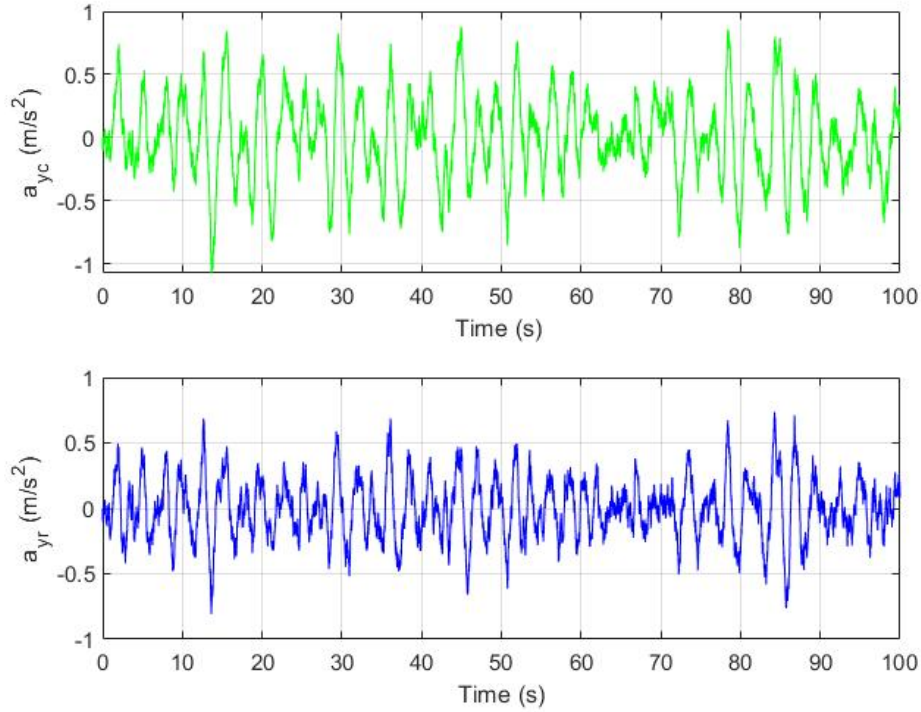

Figure 3.3: Time response of the lateral acceleration for the controlled(a_{yc}) & reduced system(a_{yr})

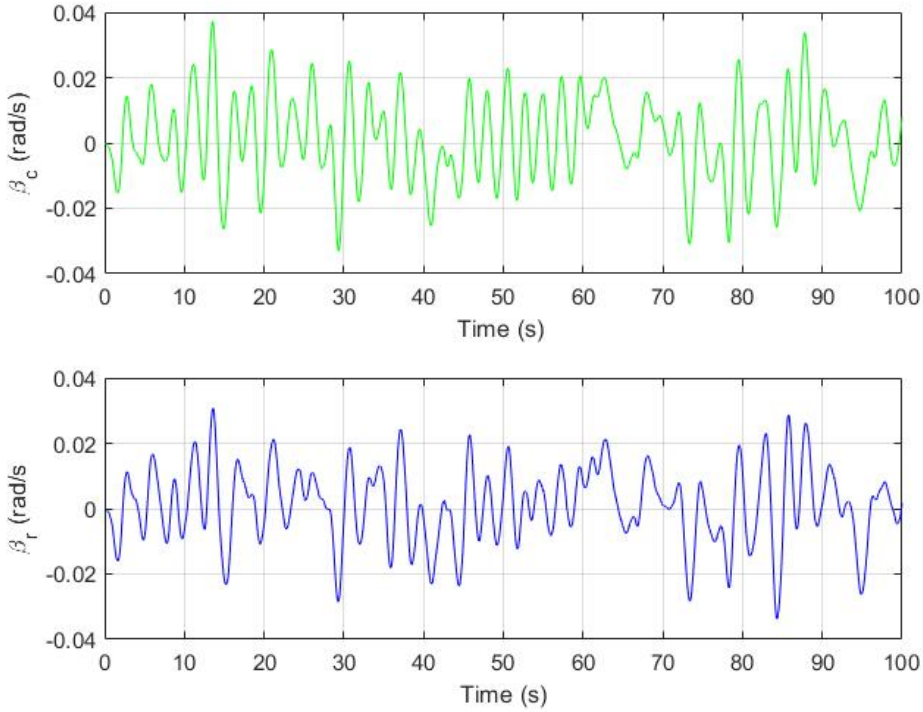

Figure 3.4: Time response of the slideslip(β) for the controlled(β_c) and reduced(β_r) system

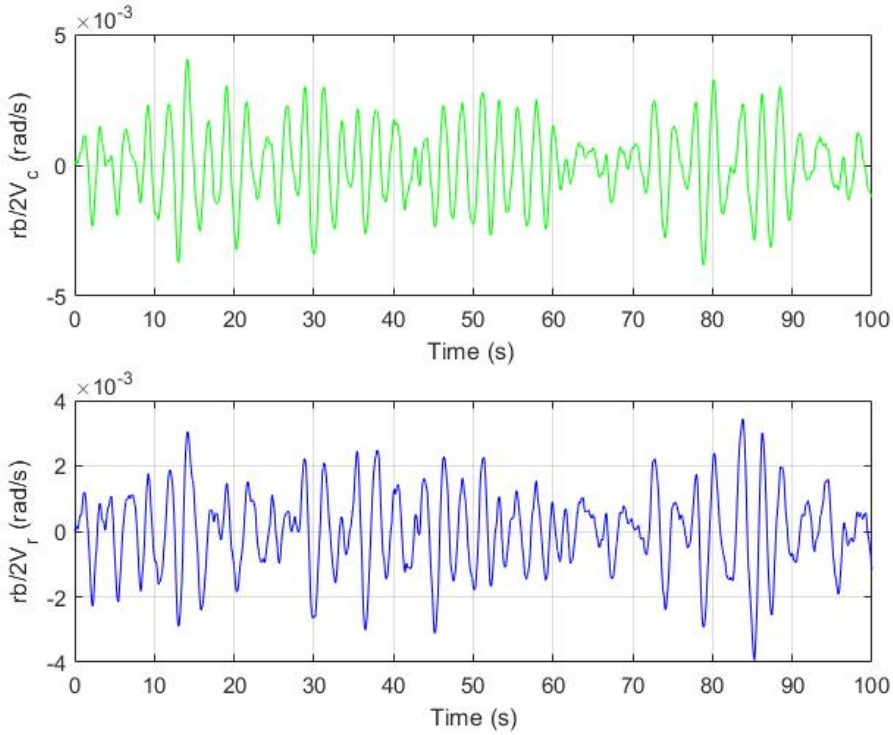

Figure 3.5: Time response of rb/2V for the controlled($rb/2V_c$) and reduced($rb/2V_r$) systems

Chapter 4

Spectral Analysis

The power spectral density(PSD) of the state variables Equation 2.12 and lateral acceleration Equation 3.1 are determined using three methods as follows:

1. Analytical method
2. Experimental method
3. Welch method

The power spectral density can be defined as the time average of the power as the function of frequency [1]. The analytical PSD is calculated by taking the average of the frequency magnitude ($\bar{A}(\omega)$) over the sampled period T.

$$S_{\bar{x}\bar{x}} = \lim_{T\to\infty} \frac{1}{2T}|\bar{A}(\omega)|^2 \tag{4.1}$$

The bode plot is used to get the magnitude of the state variables using the MATLAB function ***bode***. From the bode plot, the frequency for each variable is derived and the magnitude of it is calculated and time average is taken to determine the analytical power spectral densities.
The second method is the experimental method of Fast Fourier Transform(FFT) and is done by using the MATLAB function ***fft***. The PSDs can be directly computed, hence taking up less time. For that, the time series data $\bar{x}[n]$ is needed to calculate the DFT over the N sample.

$$\bar{X}[k] = \sum_{n=0}^{N-1} \bar{x}[n]^{-jk\frac{2\pi}{N}n} \quad for\ k\ =\ 1,\ 2, ..., N-1 \tag{4.2}$$

The periodogram can be obtained by getting the magnitude of $\bar{X}[k]$:

$$I_{Nxx}[k] = \frac{1}{N}|\bar{X}[k]|^2 \tag{4.3}$$

In order to convert from continuous time to discrete time , a scaling of $\frac{1}{dt}$ was used hence to get it back to the continuous time , a further scaling of dt is multiplied with the FFT and finally the magnitude is divided with the total period to obtain the periodogram. The last method used is the welch method and is done by implementing the MATLAB function ***pwelch***.It uses averaged periodograms to reduce the variance.The time series variable for the m^{th} window is obtained by:

$$x_m[n] = x[n + mR]w[n]\ for\ m = 0, 1, ..., N-1 \tag{4.4}$$

$$P_{x_m,M}(\omega_k) = \frac{1}{M}\left|\sum_{n=0}^{N-1} x_m(n)e^{-j2\pi nk/N}\right|^2 \tag{4.5}$$

$$S_{xx}(\omega) = \frac{1}{K}\sum_{m=0}^{K-1} P_{x_m,M}(\omega_k) \tag{4.6}$$

The notation R is the window size and K is the total number of window available.The Equation 4.5 give the periodogram for the m^{th} window and Equation 4.6 calculates the PSD over an average of K windows.
It can be noted that the PSDs calculated using the analytical method are straight lines without any fluctuations. The analytical method is deterministic and thus not very useful. On the other hand, the experimental method has a lot of fluctuations and is not smooth. For most of the state variables, deviations can be seen from the analytical PSDs because of leakage. Leakage happens when a signal cannot fit an integral number of times inside the sampling period. The PSDs determined using the welch method are comparatively smooth in nature. The leakage is mitigated in the welch method by the method of windowing.

The PSDs of sideslip for both the controlled and reduced systems are shown in Figure 4.1. For the analytical PSD, it can be observed that the initial value and slope for both systems are the same. However, in the higher frequencies, the experimental and the smooth periodogram has a less slope than the analytical PSDs. However, the slope of the smoothed PSD changes a bit faster than the experimental one. A similar trend can be observed in the PSDs of ϕ and $\frac{pb}{2V}$ in Figure 4.2. However, the change of slope is much steeper for ϕ. For $\frac{pb}{2V}$ the analytical, experimental, and smoothed PSDs have almost similar slopes. The experimental and smoothed PSDs of $\frac{rb}{2V}$ in Figure 4.3 also deviate from the analytical one at the higher frequencies.

One of the reasons why the slope changes can be the order of the system. The higher the order, the steeper will be the slop of the PSD. However, in this case, the system remains fixed thus the change in the slope cannot be justified by the order of the system. The error can be attributed to the error in the phases of the state variables at higher frequencies only. The error occurs at the Nyquist frequency. If the bode plots of β and $\frac{rb}{2V}$ in Figure 4.5 and Figure 4.6 is observed, it is seen that at higher frequencies there is a sudden change in the phase. This deviation is caused by time delay. Time delay is half of the sampling time dt. Thus the deviations of the experimental and smoothed PSDs can be attributed to the phase error and time delay.

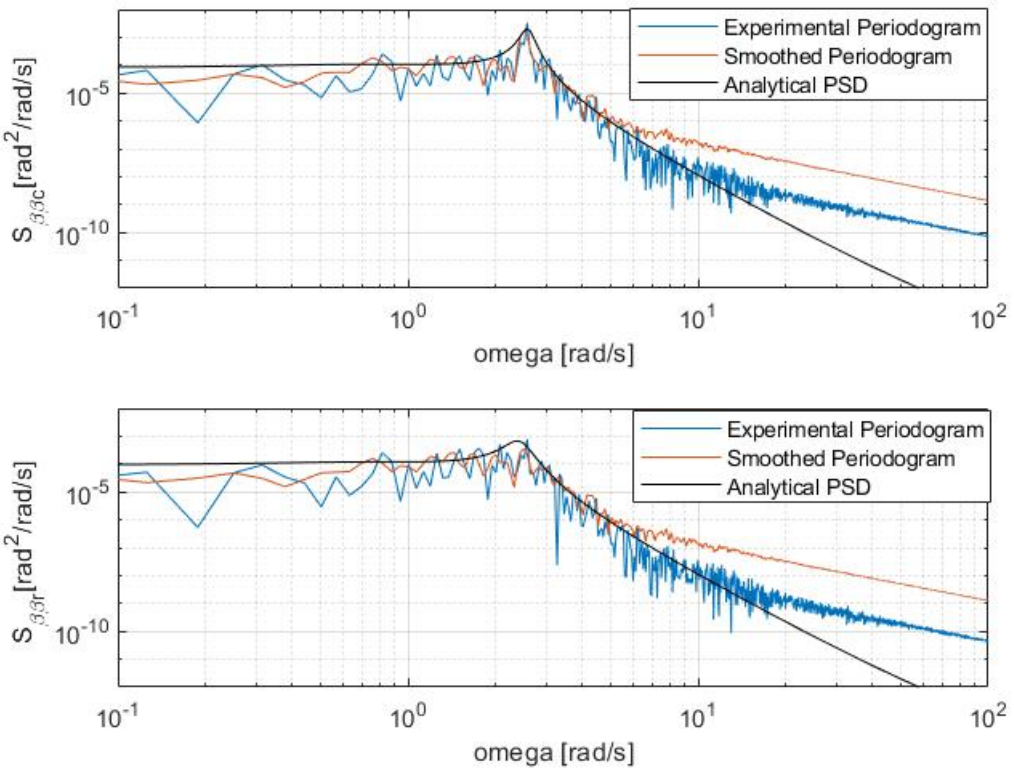

Figure 4.1: PSD of β for both controlled(β_c) & reduced(β_r) systems

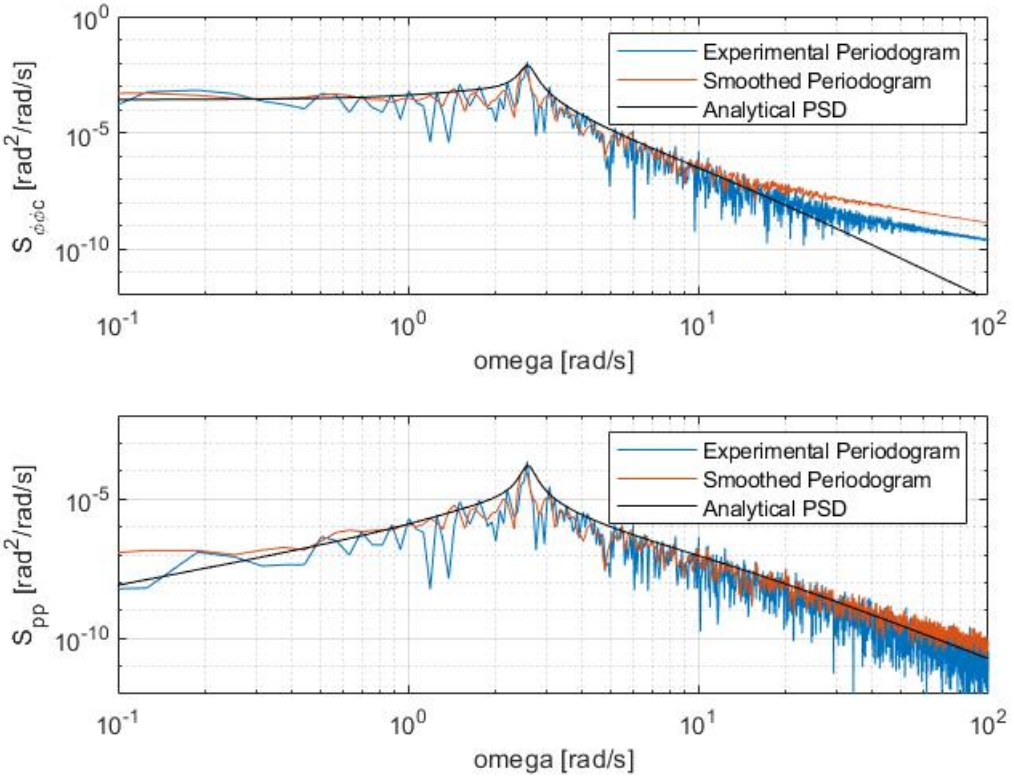

Figure 4.2: PSD of ϕ & $\frac{pb}{2V}$ for both controlled systems

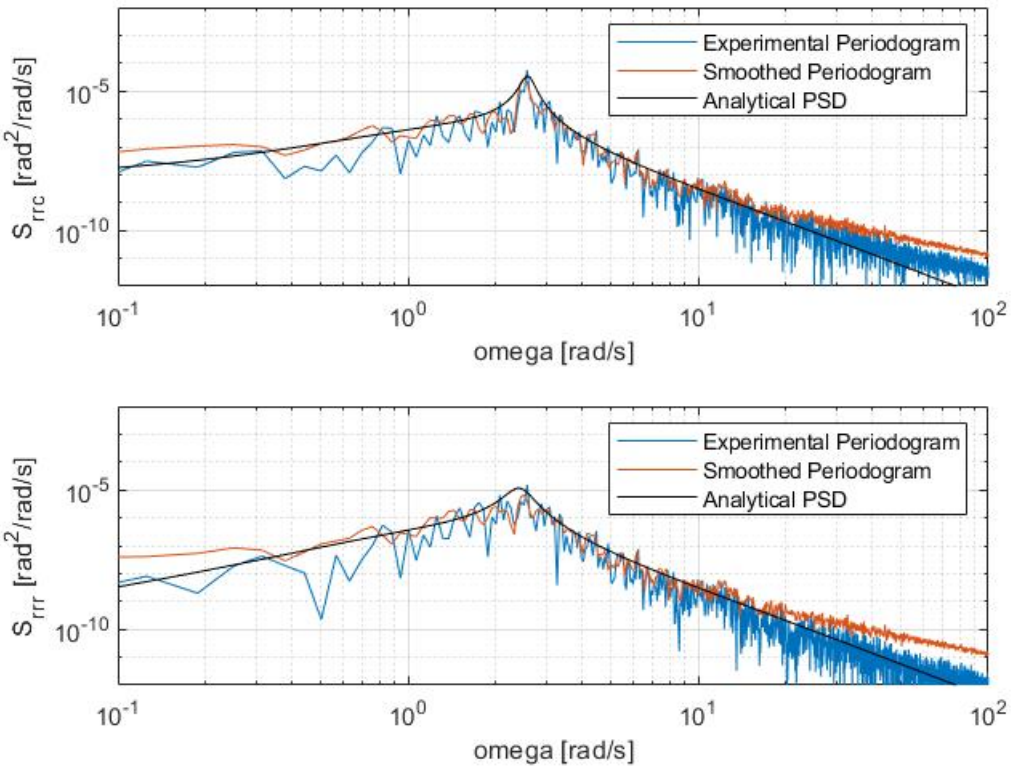

Figure 4.3: PSD of $\frac{rb}{2V}$ for both controlled($\frac{rb}{2V}_c$) & reduced($\frac{rb}{2V}_r$) systems

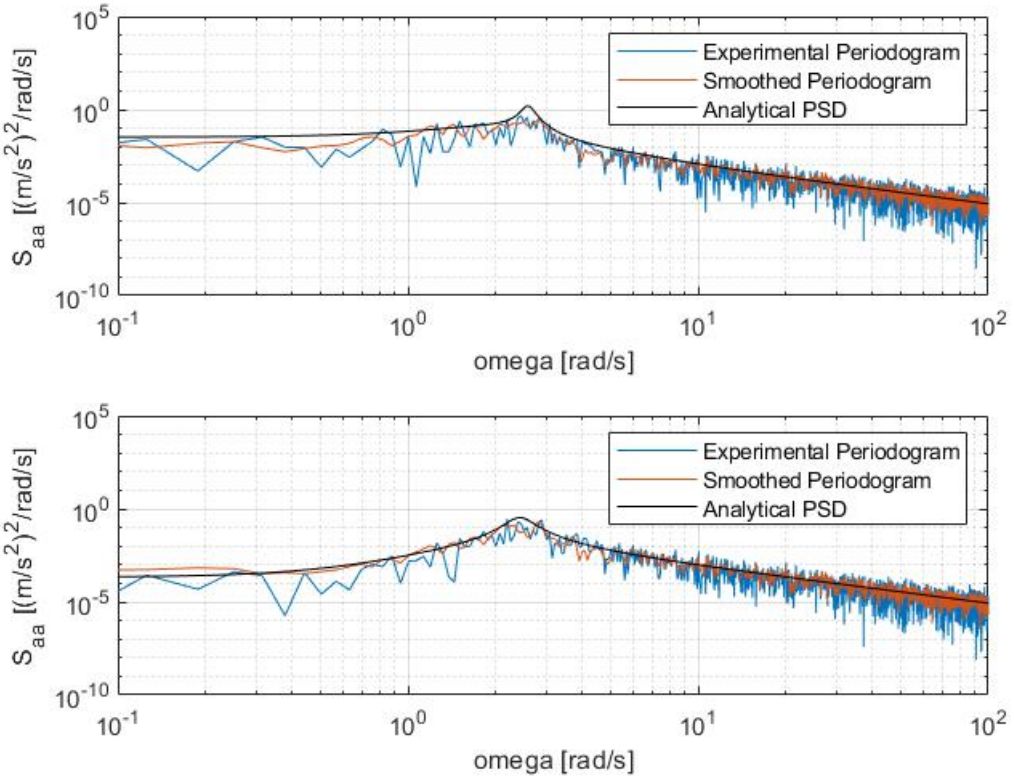

Figure 4.4: PSD of lateral acceleration for both controlled system

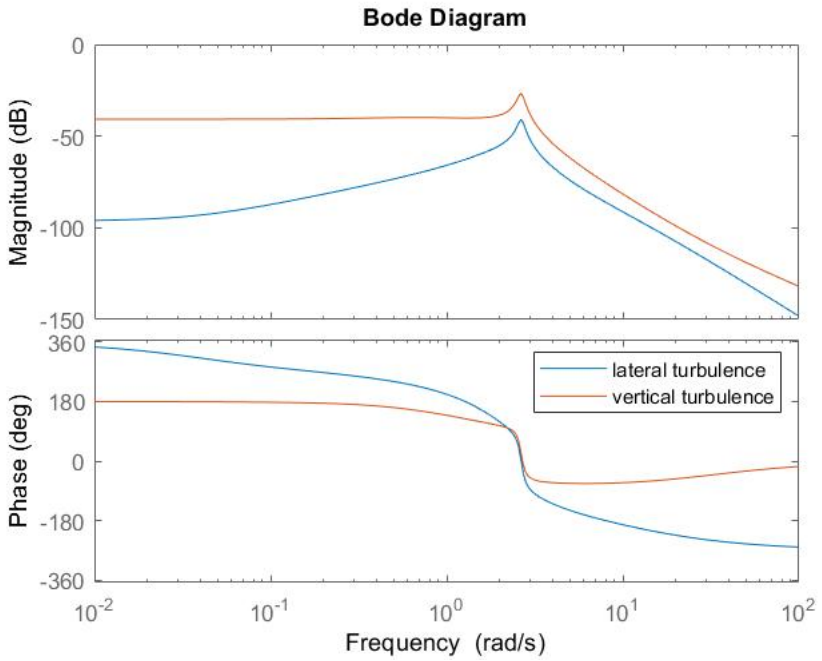

Figure 4.5: Bode plot for the lateral and vertical turbulence of β

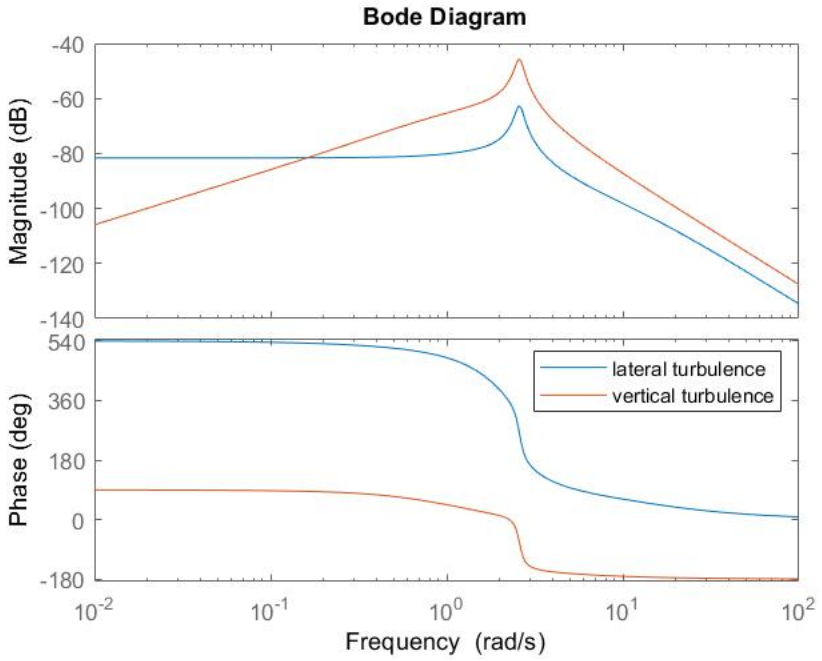

Figure 4.6: Bode plot for the lateral and vertical turbulence of $\frac{rb}{2V}$

Chapter 5

Variance Calculation

This chapter discusses about the variance calculation of the state variables and the lateral acceleration. The variance is calculated using three methods:

- Analytical Power Spectra
- Lyapunov Equation
- MATLAB routine ***var.m***

The variance of the analytical power spectra is calculated by integrating the analytical PSD value. A scaling of $1/\pi$ is done. The analytical variance is given by:

$$\sigma_x^2 = \frac{1}{\pi}\int_0^\infty S_{xx}(\omega)d\omega \tag{5.1}$$

So the analytical power spectra variance is essentially the area under the curve. The values of the PSDs are taken from the calculations of chapter 4. The other method used to calculate the variance is the Lyapunov equation Equation 5.2. The A and B are the state spaces taken from chapter 2. The C_{xx} is the auto-covariance of the state vectors mentioned in chapter 2. The values of the variances are situated along the diagonal of C_{xx}. The W is an identity matrix constructed using the Matlab command ***eye(2,2)***.

$$A.C_{xx} + C_{xx}.A^T + B.W.B^T = 0 \tag{5.2}$$

The last method is using the MATLAB function ***var***. Matlab uses the following equation:

$$\sigma_x^2 = \frac{1}{N-1}\sum_{i=1}^{N}|X_i - \mu_x|^2 \tag{5.3}$$

$$\mu_x = \frac{1}{N}\sum_{i=1}^{N}X_i \tag{5.4}$$

In Equation 5.4 the mean of the variables is calculated over the total sample size. From that variance is calculated in Equation 5.3.In one way the var.m also calculated the area under the curve.

The calculated variances for both the complete and reduced models are shown in Table 5.1 and Table 5.2. If the states β and $\frac{rb}{2V}$ of both the models are compared, a difference can be a notice in all three methods. We know variance essentially calculates the area under the curve. It can be noticed from the Figure 4.1, Figure 4.3 and Figure 4.4 that the area under the curve for the reduced model is smaller than the complete model and this explains why the variances of the states for the reduced model is lower. The difference in area is due to the pole placements of the two model as seen in Table 2.1

State variables	Analytical power spectra	var.m	Lyapunov
$\beta\ rad^2$	3.2520e-04	2.8938e-04	2.5943e-04
$\phi\ rad^2$	0.00143	8.1959e-04	8.355e-04
$\frac{pb}{2V}\ rad^2$	2.4359e-05	1.4148e-05	1.4481e-05
$\frac{rb}{2V}\ rad^2$	4.8175e-06	3.8851e-06	3.6985e-06
$a_y\ m^2/s^4$	0.2758	0.1948	0.1843

Table 5.1: Variances of the state variables for the complete model

State variables	Analytical power spectra	var.m	Lyapunov
$\beta\ rad^2$	2.1518e-04	2.0643e-04	1.788e-04
$\frac{rb}{2V}\ rad^2$	2.7763e-06	2.4646e-06	2.2507-06
$a_y\ m^2/s^4$	0.0883	0.0774	0.0731

Table 5.2: Variances of the state variables for the reduced model

Differences can also be found among the results of the different methods. The analytical method calculates the variance from the analytical PSD. The analytical PSD is constructed using the Bode plots of the state variables to the vertical and lateral turbulence inputs. The analytical curve has almost not fluctuations, hence the area under it can be calculated uniformly. The inputs for the var.m method is derived from the system output after using the ***lsim*** command on the state space matrices with inputs for the lateral and vertical turbulence. The inputs have a lot of noise associated with them which also results in a crude approximation of the area which results in the difference of the variances between the analytical and var.m methods. The same kind of approximation happens in the Lyapunov method and hence it can be noticed that the difference between the var.m and Lyapunov are very less. The results of the two methods almost become similar over an extended time.

Chapter 6

Conclusion

The report analyzed the effect of asymmetrical atmospheric turbulence on a rigid aircraft, focusing on the vertical and lateral gust components. In chapter 2 the full and the reduced aircraft models were analyzed to determine if they are stable. It was found that the full model was not completely stable, hence a roll damper was introduced and a stable system was derived. The reduced model was already stable so no modification was made.

In chapter 3 both the full stable model and the reduced model were simulated over some time of 600 s to get the time behavior of the system state variables. The time-domain analysis data of the states were then used for the spectral analysis and variance calculations. The time-domain simulations of the gust components were not shown, but they also influence the whole system. The spectral analysis of all the derived states was performed in chapter 4. The methods; analytical, experimental, and welch were used to derive the PSDs for all the states and the lateral acceleration. The outcome of each method varied from the other methods and the reasons behind the variations were adequately explained alongside the results. It also has to noted that the experimental methods and the welch method have significant deviations at the higher frequencies from the analytical method, the reason was traced back to the time delay and phase error.

Ultimately, the variances of all the state variables and the lateral acceleration component were determined. We again used three different methods; analytical, var.m, and Lyapunov's equations to determine the variances. It was seen that with the increase of period, the variances from Lyapunov and var.m become similar.However the simulation can give varied results in the variances to some extent due to the randomisation taken into account while constructing the gust components in chapter 3.

The main goal of the assignment was to analyze how systems get affected by real-life phenomenons. The outcome was to get familiarised with the analysis of stochastic processes in both time and frequency domains. Though the system analyzed here was an aircraft model, the knowledge and the methods used can be applied to any real-world system.

Bibliography

[1] J. C. Van Staveren W.H.J.J. Chu Q.P. Mulder M. Mulder, J. A. Van der Vaart. Aircraft responses to atmospheric turbulence. lecture notes ae4304., October 2020.

[2] W.H.J.J. Van der Vaart J.C. De Weerdt E Mulder, J. A. Van Staveren. Flight dynamics. lecture notes ae3302., October 2020.